Results and forecasts on cosmic inflation from weak lensing

Agnès Ferté[1] and Kevin Hong[1,2]

[1]*SLAC National Accelerator Laboratory, Menlo Park, California 94025, USA*
[2]*Department of Physics and Astronomy, 430 Portola Plaza, University of California, Los Angeles, California 90095, USA*

(Received 9 October 2023; accepted 14 March 2024; published 1 May 2024)

We highlight the role of weak lensing measurements from current and upcoming stage-IV imaging surveys in the search for cosmic inflation, specifically in measuring the scalar spectral index n_s. To do so, we combine the Dark Energy Survey 3 years of observation weak lensing and clustering data with Bicep/*Keck*, *Planck*, and Sloan Digital Sky Survey data in $r\Lambda$CDM (cold dark matter) where r is the tensor-to-scalar ratio. While there is no significant improvement in constraining power, we obtain a 1σ shift on n_s. Additionally, we forecast a weak lensing and clustering data vector from the 10-year Legacy Survey of Space and Time by the Vera C. Rubin Observatory and show its combination with current data would improve their n_s constraints by 25% in $r\Lambda$CDM.

DOI: 10.1103/PhysRevD.109.103502

I. INTRODUCTION

In the ΛCDM model, scalar perturbations of the metric have been evolving since cosmic inflation, sourcing the large-scale structures in the recent Universe. Their primordial power spectrum $P_{\mathcal{S}}(k)$ follows:

$$P_{\mathcal{S}}(k) = A_s \left(\frac{k}{k_s}\right)^{n_s-1}, \tag{1}$$

with A_s the amplitude of scalar pertubation, k the wave number, k_s the wave number at a pivot scale, set to 0.05 Mpc^{-1} in this analysis, and n_s the scalar spectral index.

The implications of cosmic microwave background (CMB) measurements for inflationary search were introduced in [1–3]. And indeed, since then, one of the successes of the last generation of CMB experiments was measuring n_s different from unity at high significance (8σ in [4]) thus excluding a scale-invariant primordial power spectrum, a key step towards establishing inflation. Now and over the coming decade, CMB polarization experiments aim at detecting large scale B modes to constrain the tensor-to-scalar ratio r, the energy scale of inflation. Today, the Bicek/*Keck* experiment in combination with CMB *Planck* and baryonic acoustic oscillation (BAO) measurements from 6dFGS, Main Galaxy Sample (MGS) and Baryon Oscillation Spectroscopic Survey (BOSS) DR12 data constrain r to be below 0.036 at 95% confidence [5]. In the future, the *LiteBIRD* satellite [6], the Simons Observatory [7], and CMB-S4 [8] ground-based experiments will aim at attaining $\sigma(r) \sim 10^{-3}$.

In parallel, a new generation of photometric galaxy surveys will soon start mapping galaxies to further test the ΛCDM model with the goal of understanding the origin of the current cosmic acceleration. On the ground, the Vera C. Rubin Observatory will produce the Legacy Survey of Space and Time (LSST) [9,10], a 10-year imaging survey of half the celestial sphere, while the Euclid [11] and Roman [12] satellites will image galaxies from space. One of their main objectives is to probe dark energy and modified gravity, through the evolution of the background and structures in the recent Universe through various observables [13–16]. Weak gravitational lensing is especially promising as being one of the few unbiased probes of dark matter distribution and having been successfully used for precision cosmology with stage-III experiments [17–19]. Weak lensing is mostly sensitive to the energy density of matter Ω_m and the variance of matter fluctuations σ_8, however with improved measurements from stage-IV surveys (as defined in [20]), weak lensing will become more sensitive to other properties of the matter power spectrum: in this paper, we investigate the role of weak lensing in inflationary search, especially through its sensitivity to the scalar spectral index n_s. Weak lensing indeed brings complementary information from CMB, by accessing different modes, in the range $k \sim [0.1, 5]\ h/\mathrm{Mpc}$, compared to the range accessed by the CMB $k \sim [10^{-4}, 10^{-1}]\ h/\mathrm{Mpc}$. We note that in parallel, galaxy surveys will also aim at detecting primordial non-Gaussianities, through galaxy clustering as forecasted in [21–23], as well as through weak lensing [24] and alignment of galaxies [25].

There are now a few indications that weak lensing could bring promising improvements on n_s constraints. In [26], the second moment of the mass map from the Dark Energy Survey shows sensitivity to n_s. Additionally, [27,28] indicate significant constraints on n_s with stage-IV surveys,

although they are probably partly informed by prior choices. Weak lensing was also used in [29] to determine the sensitivity of *Euclid*-like surveys in detecting specific features arising from inflation. Furthermore, [30] shows that future spectroscopic surveys such as *Euclid* will increase the constraints in the n_s direction by close to a factor of 2 in $r\Lambda$CDM. However, this analysis did not consider weak lensing, so we complete the picture in the present paper by considering information from photometric surveys, specifically the Dark Energy Survey (DES) and the future LSST. To do so, we first infer cosmology in ΛCDM and $r\Lambda$CDM using data from the DES 3 years of observation (DES Y3) and second, from our predicted 10-year LSST data vector. We describe both datasets in Sec. II A and detail the other likelihoods used as well as our parameter estimation approach in Sec. II B. We show our results in ΛCDM and $r\Lambda$CDM models in Sec. III. We finally conclude in Sec. IV with outlooks on weak lensing's role in inflation search.

II. ANALYSIS

A. DES Y3 and predicted LSST Y10 weak lensing and clustering

To quantify weak lensing contributions to constraints on inflation, we choose to combine information from weak lensing and clustering in order to pin down systematics such as intrinsic alignment and galaxy bias as done in [17–19]. Their statistics are summarized in the form of three correlation functions in tomographic bins (referred to as 3×2 pt): cosmic shear $\xi_\pm(\theta)$ corresponding to the correlations of galaxy shapes, galaxy-galaxy lensing $\gamma_t(\theta)$, the tangential shear of background galaxies around lens galaxies, and finally clustering $w(\theta)$ corresponding to the correlation of lens galaxy positions. We use DES Y3 3×2 pt along with the modeling choices and angular scale cuts used in DES Y3 cosmological analysis in [17]. We tested that adding the DES Y3 shear ratio likelihood from [31] did not change the results.

To forecast weak lensing from stage-IV surveys, we simulate a data vector from the 10 years of LSST (hereafter LSST Y10). For simplicity, in this case, we choose to use angular power spectra in harmonic space C_ℓ^{ab} (with a and b either the convergence field κ or the density δ) as our summary statistics. We closely follow the choices made in [13], which we will refer to as the SRD (the LSST-Dark Energy Survey Science Collaboration Science Requirement Document), with small changes for more realistic forecasts which we describe below.

Regarding LSST Y10 observations, we set the observed sky fraction used to create the source and lens samples to be 35% of the celestial sphere. The redshift distribution $n(z)$ of both samples is described by a Smail distribution, i.e.,

$$n(z) = z^\alpha e^{(-z/z_0)^\beta}. \tag{2}$$

TABLE I. Parameters used to model the redshift distribution of the lens and galaxy samples [see Eq. (2)], along with the number of redshift bins, effective number density $n_{\rm eff}$ and shape noise σ_ϵ used to simulate a LSST Year 10 weak lensing and clustering data vector, following [13].

Parameters	Source sample	Lens sample
α	2	2
z_0	0.11	0.28
β	0.68	0.9
Number of redshift bins	5	10
$n_{\rm eff}$ (in arcmin^{-2})	27	48
σ_ϵ	0.26	

Parameters α, β, and z_0 of this distribution along with the number of redshift bins, effective number density, and shape noise are summarized in Table I, following the SRD.

We list below the choices made to model the LSST Y10 C_ℓ data vector:

(1) The matter power spectrum is computed using CAMB [32–35]. As the SRD uses scales down to $\ell_{\rm shear}=3000$, we decided to add a nonlinear prescription with baryonic feedback from HMCode-2020 [36] to model the small angular scales more realistically. We set $\log_{10}(T_{\rm AGN}/K)=7.8$ inside the range recommended in [36], with $T_{\rm AGN}$ corresponding to the strength of Active Galactic Nuclei feedback in simulations.

(2) The intrinsic alignment (IA) of galaxies is modeled using the nonlinear alignment model [37] such that the IA contributions to cosmic shear are linearly related to the nonlinear matter power spectrum, where the amplitude of IA has $(1+z)$ redshift dependence as used in DES Year 1 [38].

(3) Similarly to the SRD, we adopt a linear galaxy bias model parametrized by a bias parameter per redshift bin.

We use CosmoSIS [39] to model and analyze DES Y3 and our LSST Y10-like data vector. We thus theoretically predict the expected C_ℓ, with a Gaussian covariance matrix computed within CosmoSIS. Weak lensing analyses such as [17] remove measurements, typically at small angular scales, where the modeling is uncertain. We do similarly and follow the guidelines from the SRD, thus using $\ell_{\rm max}=3000$ for weak lensing, and $k_{\rm max}=0.3\ h/{\rm Mpc}$ for the clustering part of the data vector. We translate this value into corresponding $\ell_{\rm max}$ for each lens redshift bins as shown in Table II.

The effect of the scalar spectral index n_s on shear power spectrum in redsfhit bin 2 is shown on the top panel of Fig. 1 along with the predicted data points and error bars from LSST Y10. The tilt of the primordial power spectrum translates into a dampening at low-ℓ (of at most 3% for $n_s=0.98$) and a boost at higher ℓ. Given the shown error bars, we thus expect LSST Y10 weak lensing to have

TABLE II. Harmonic-space scale cuts adopted in the present analysis following [13], i.e., $\ell_{\rm max} = 3000$ for shear and $k_{\rm max} = 0.3\ h/{\rm Mpc}$ for correlations involving the lens sample. The total number of data points used is 513.

Lens bin	1	2	3	4	5	6	7	8	9	10
$\langle z_\ell \rangle$	0.27	0.46	0.61	0.74	0.88	1.03	1.20	1.42	1.73	2.45
$\ell_{\rm max}$	227	370	466	550	629	708	791	884	1000	1210

sensitivity to this parameter. We however also show the effect of the amplitude of scalar perturbations A_s on the lower panel of Fig. 1, which behaves similarly to n_s on small angular scales, where the sensitivity is best. This translates into a degeneracy between the two parameters which is shown in the contours from analyzing our LSST Y10 3×2 pt data dector in ΛCDM in Fig. 4. For similar reasons, the baryonic feedback parameter $T_{\rm AGN}$ is degenerate with n_s while the energy density of baryons Ω_b and the Hubble parameter H_0 are anticorrelated with n_s. We therefore need to combine LSST Y10 with other data such as *Planck* temperature and polarization power spectra to break such degeneracy, which we do in the following section.

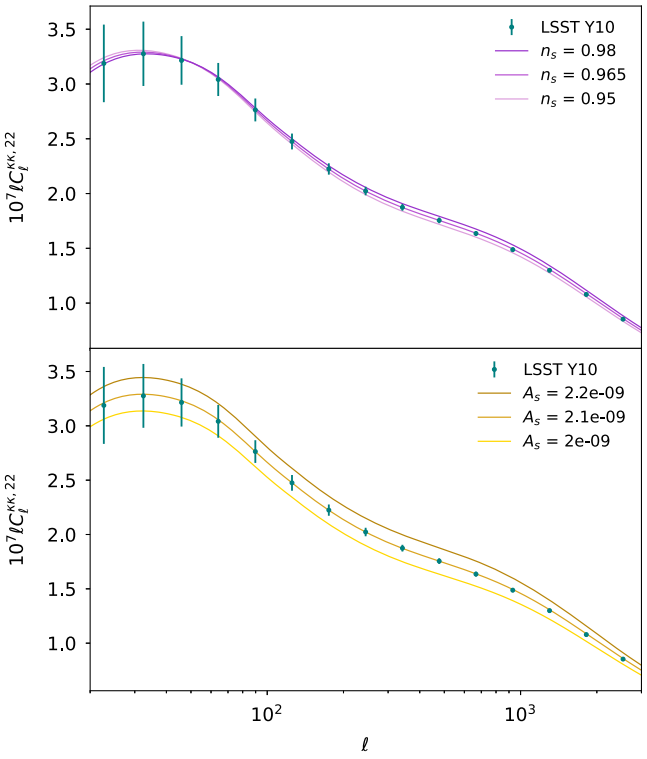

FIG. 1. Theoretical predictions of the shear angular power spectra in redshift bin 2 of the LSST Y10 source $n(z)$ for three values of the scalar spectral index n_s in the top panel, and three values of the amplitude of scalar perturbations A_s in the lower panel, along with our forecasted LSST Year 10 shear data vector and error bars.

B. Other datasets and likelihood analysis

We adopt a Bayesian approach, where we sample the posterior using the NAUTILUS importance nested sampler [40] within CosmoSIS. The parameter estimation is made in ΛCDM to forecast the sensitivity of LSST Y10 on n_s and in rΛCDM to forecast implications of DES Y3 and LSST Y10 for cosmic inflation.

Although our LSST Y10 data vector is a theoretical prediction, we combine it with current real CMB and BAO data while of course measurements of such observables will also become more precise in the coming decade. We indeed want to show results in the current experimental landscape first, using weak lensing data from DES Y3 in rΛCDM and then show how solely improving DES Y3 to LSST Y10 would translate into inflation constraints. We thus use *Planck* 2018 temperature, polarization E modes and lensing potential ϕ power spectra in the form of the TT, TE, EE *lite* high-ℓ, EE, and TT low-ℓ as well as lensing likelihoods, to add information on the cosmological parameters [4]. We refer to this combination as TTTEEE + low-ℓ + lensing. Additionally, to inform the geometry of the Universe and break the degeneracy between σ_8, Ω_m, and the Hubble parameter H_0, we add Baryonic Acoustic Oscillation measurements from the Sloan Digital Sky Survey. They specifically include likelihoods on distance measurements from the MGS [41], the BOSS DR12 [42] reanalyzed in [43] and extended Baryon Oscillation Spectroscopic Survey (eBOSS) DR16 measurements from luminous red galaxies [44,45], emission line galaxies [46], quasars [47,48], and Ly-α forest [49].

In rΛCDM, we additionally include the likelihood on the tensor-to-scalar ratio r from Bicep/*Keck B* modes power spectrum measurements from [5] (hereafter BK18). We note that Fig. 3 shows in coral the combination of BK18, Planck TTTEEE + low − ℓ + lensing and SDSS including eBOSS DR16, while BK18 analysis in [5] uses 6dFGS, MGS, and BOSS DR12. The shift in n_s caused by this update in the BAO measurement is not significant (0.07σ).

Table III summarizes the parameters varied and their corresponding priors, including both cosmological and nuisance parameters. We use GetDist [50] to quote constraints on parameters as the mean and 68% credible intervals in one dimension, and to show the 68% and 95% credible regions in two dimensions.

III. RESULTS, FORECASTS, AND IMPLICATIONS FOR INFLATION

In Fig. 2, we summarize the present status of n_s measurements in ΛCDM, quoting results from Wilkinson microwave anisotropy probe (WMAP) data, the first rejection of $n_s = 1$ at high significance in [51,52], and the tightest current measurements from the *Planck* satellite [4] as well as the results from DES Y3 combined with *Planck* (which does not include CMB lensing) as published in [17]. We then

TABLE III. Priors on parameters used in the parameter estimation, where brackets indicate flat priors while $\mathcal{G}(m,\sigma)$ indicates a Gaussian prior of mean m and standard deviation σ.

Parameters	Priors
Cosmology	
A_s	$[0.5, 5]\times10^{-9}$
n_s	$[0.88, 1]$
Ω_m	$[0.1, 0.7]$
Ω_b	$[0.03, 0.07]$
h_0	$[0.55, 0.9]$
r (in $r\Lambda$CDM)	$[0, 0.2]$
DES Y3	
See Table 1 in [17]	
Forecast LSST Y10	
$\log(T_{\rm AGN})$	$[7.7, 8.0]$
$A_{\rm IA}$	$[-5, 5]$
α	$[-5, 5]$
$m_i, i\in[1,5]$	$[-0.005, 0.005]$
$\Delta z^i_s, i\in[1,5]$	$[-0.01, 0.01]$
$\Delta z^i_\ell, i\in[1,10]$	$[-0.01, 0.01]$
$b_i, i\in[1,10]$	$[1.9, 2.1]$
Planck	
τ	$[0.01, 0.8]$
$A_{\rm Planck}$	$\mathcal{G}(1, 0.0025)$

report the mean and 68% credible interval on n_s we obtain from our analysis of LSST Y10 3×2 pt alone and LSST Y10 3×2 pt combined with *Planck* TTTEEE + low-ℓ + lensing in orange. While LSST Y10 by itself does not result in competitive results on the spectral index, the forecast shows a 30% improvement on n_s from adding LSST Y10 to *Planck* compared to *Planck* alone. Although the gain in constraining power on n_s expected from spectroscopic surveys is greater [30], weak lensing and clustering prove to be useful additions as probes of the matter power spectrum. In Fig. 4 in the Appendix, we show the predicted constraints on cosmology from LSST Y10 3×2 pt in red as well as the combination with *Planck* in dark blue.

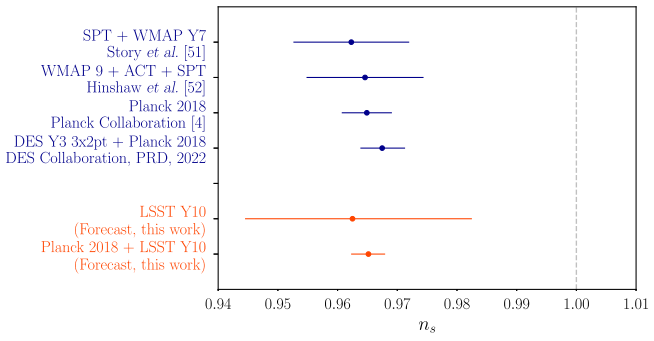

FIG. 2. Past and current measurements of the scalar spectral index n_s in blue along with the predictions from our forecasted LSST Year 10 weak lensing and clustering data vector, alone and in combination with *Planck* TTTEEE, low-ℓ and lensing likelihoods in orange.

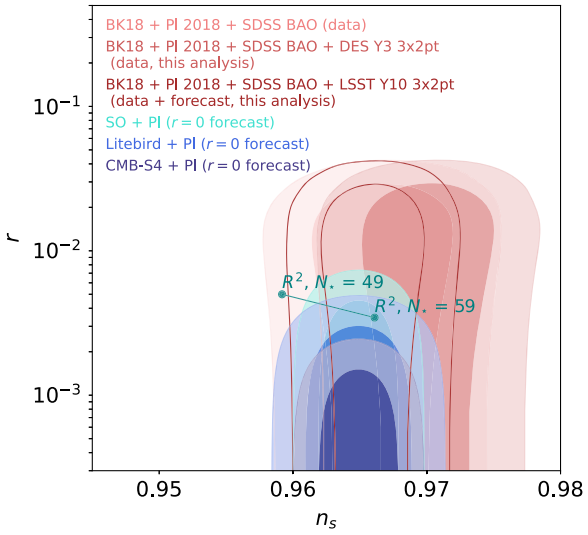

FIG. 3. Current constraints and forecasts on the tensor-to-scalar ratio r and the scalar spectral index n_s using the likelihood on r from Bicep/*Keck* in addition to *Planck* 2018 TTTEEE, low-ℓ and lensing likelihoods, BAO measurements from SDSS, in salmon. We add DES Y3 weak lensing and clustering data to this fiducial data combination, and show the results in red. Forecasts from replacing DES Y3 by our LSST Y10-like weak lensing and clustering data vector is shown in brown. We also show for reference forecasts for future stage-IV CMB experiments: Simons Observatory (in turquoise), *LiteBIRD* (in blue), and CMB-S4 (in dark blue), with the prediction from Starobinsky inflationary model (referred to as R^2 model) for e-fold $N_\star$ between 49 and 59 overlaid in teal.

We now turn to the implications of such improvements on inflationary models, in $r\Lambda$CDM. The results from our parameter inference are summarized in Fig. 3 where we show constraints in the (r,n_s) plane, using the BK18 likelihood on the tensor-to-scalar ratio in addition to *Planck* TTTEEE + low-ℓ + lensing and SDSS BAO measurements in salmon. As a reference, we also show predictions from the Starobinsky model [53,54] for e-folds $N_\star$ between 49 and 59 in teal. As nicely summarized in [52], r and n_s are indeed simply related to the number of e-folds in the super-horizon limit, following [55]. In particular, $n_s-1=-2/N_\star$.

First, adding DES Y3 3×2 pt results in the red contour on (r,n_s). There is virtually no improvement on n_s but strikingly, the contours are shifted by 1σ to higher values of n_s, indicating that any e-folds $N_\star$ below 55 are rejected at more than 2σ. We believe this shift to be caused by the slight tension between *Planck* and DES Y3 3×2 pt, where DES Y3 pulls the results towards lower values of Ω_m which in turn translates into higher values of n_s [given the slight anticorrelation in *Planck*'s (Ω_m,n_s) plane].

We then switch DES Y3 to our predicted LSST Y10 3×2 pt data vector and report the result in brown, indicating that the 68% credible interval on n_s would in this case be improved by 25%. We note that our predicted LSST Y10 3×2 pt data vector was computed for a value of n_s equal to its mean measured by *Planck* 2018. The addition of LSST Y10 3×2 pt will thus help test the R^2 model more strongly.

In the future, stage-IV CMB experiments dedicated to inflation search will aim at $\sigma(r)\sim10^{-3}$. The combination of their polarization power spectra with *Planck* will also tighten the constrains on n_s. As a reference we show forecasts for Simons Observatory (SO) in cyan, *LiteBIRD* in light blue, and CMB-S4 in blue, taken from their forecast papers [6–8]. In future work, we will assess the expected improvements on n_s, and therefore on R^2 model constraints, from combining these experiments with future weak lensing (as shown here) and spectroscopic clustering (as shown in [30]) measurements.

IV. CONCLUSION

The detection of cosmic microwave background B modes on large scales is a great goal of modern cosmology as an awaited signal from cosmic inflation. Experiments such as BICEP/*Keck* have therefore been developed to enable the current tightest constraints on the tensor-to-scalar ratio r, with implications for inflation shown as constraints on r and the scalar spectral index n_s of scalar perturbations as shown in Fig. 3. In the coming decade, a new generation of CMB polarization experiments including Simons Observatory, *LiteBIRD*, CMB-S4 will aim at improving constraints in the r direction, by attaining $\sigma(r)\sim10^{-3}$. However, we also need improvements in the n_s direction to help further test inflationary models (such as R^2 model), in particular [30] already showed the power of spectroscopic measurements for surveys like *Euclid* in improving n_s constraints by a factor of 2. In the present analysis, we complete the picture by showing the expected improvements from current and stage-IV weak lensing surveys in inflationary search and summarize our results in Table IV.

TABLE IV. Mean and 68% credible interval on the scalar spectral index n_s in $r\Lambda$CDM from the fiducial combination of current data [(i.e., BK18 + *Planck* 2018 (TTTEEE + low-ℓ + lensing) + SDSS BAO (MGS, eBOSS DR16)] and combination with weak lensing and clustering data.

$r\Lambda$CDM	n_s
Fiducial	$0.9668^{+0.0037}_{-0.0035}$
Fiducial + DES Y3 3×2 pt	$0.9702^{+0.0034}_{-0.0035}$
Fiducial + forecast LSST Y10 3×2 pt	$0.9660^{+0.0028}_{-0.0027}$

The next steps in this direction include assessing weak lensing and clustering sensitivity to the running of the scalar index, α_s, the derivative of n_s to the wave number k as done with the Kilo Degree Survey in [56] as well as including information from the mass and galaxy maps beyond two-point statistics. Additionally, we showed results using the primordial and lensing CMB information from *Planck* but further work will be needed to understand how future galaxy surveys will help stage-IV CMB experiments in improving n_s constraints. On a similar note, we show in Fig. 5 how n_s priors informed by the CMB will impact cosmology from LSST Y10, the parameter σ_8 appearing unchanged. To conclude, given the experimental landscape of the coming decade, we will want to combine results from both spectroscopic and weak lensing surveys with CMB polarization data to perform more complete inflation searches.

ACKNOWLEDGMENTS

A. F. would like to thank Daniel Green for inputs on CMB-S4 forecasts and Judit Prat for discussions about LSST Y1 forecasts. This work was supported in part by the U.S. Department of Energy, Office of Science, Office of Workforce Development for Teachers and Scientists (WDTS) under the Science Undergraduate Laboratory Internships Program (SULI). Some of the computing for this project was performed on the Sherlock cluster. We would like to thank Stanford University and the Stanford Research Computing Center for providing computational resources and support that contributed to these research results. We thank the developers of CosmoSIS and modules therein, the parameter inference tool used in this analysis, available at this link.

APPENDIX: LSST Y10 WEAK LENSING AND CLUSTERING FORECAST

We show in Fig. 4 the credible regions of cosmological parameters obtained by analyzing our predicted LSST Y10 3×2 pt C_ℓ data vector in ΛCDM in red, from *Planck* 2018 TTTEEE + low-ℓ + lensing likelihoods in light blue and their combination with LSST Y10 in dark blue. We thus show how LSST and *Planck* combined together will improve cosmological constraints by breaking several degeneracies.

In Fig. 5, we show forecasts on A_s, n_s, and σ_8 obtained analyzing LSST Y10 3×2 pt using a flat wide prior on n_s (shown in red), a Gaussian prior informed by *Planck* 2018 (in coral) and SO (in pink). In both cases, the standard deviation of the Gaussian prior is five times the 68% credible interval from *Planck*, and five times the expected uncertainty from SO (expected to be twice as small as *Planck*).

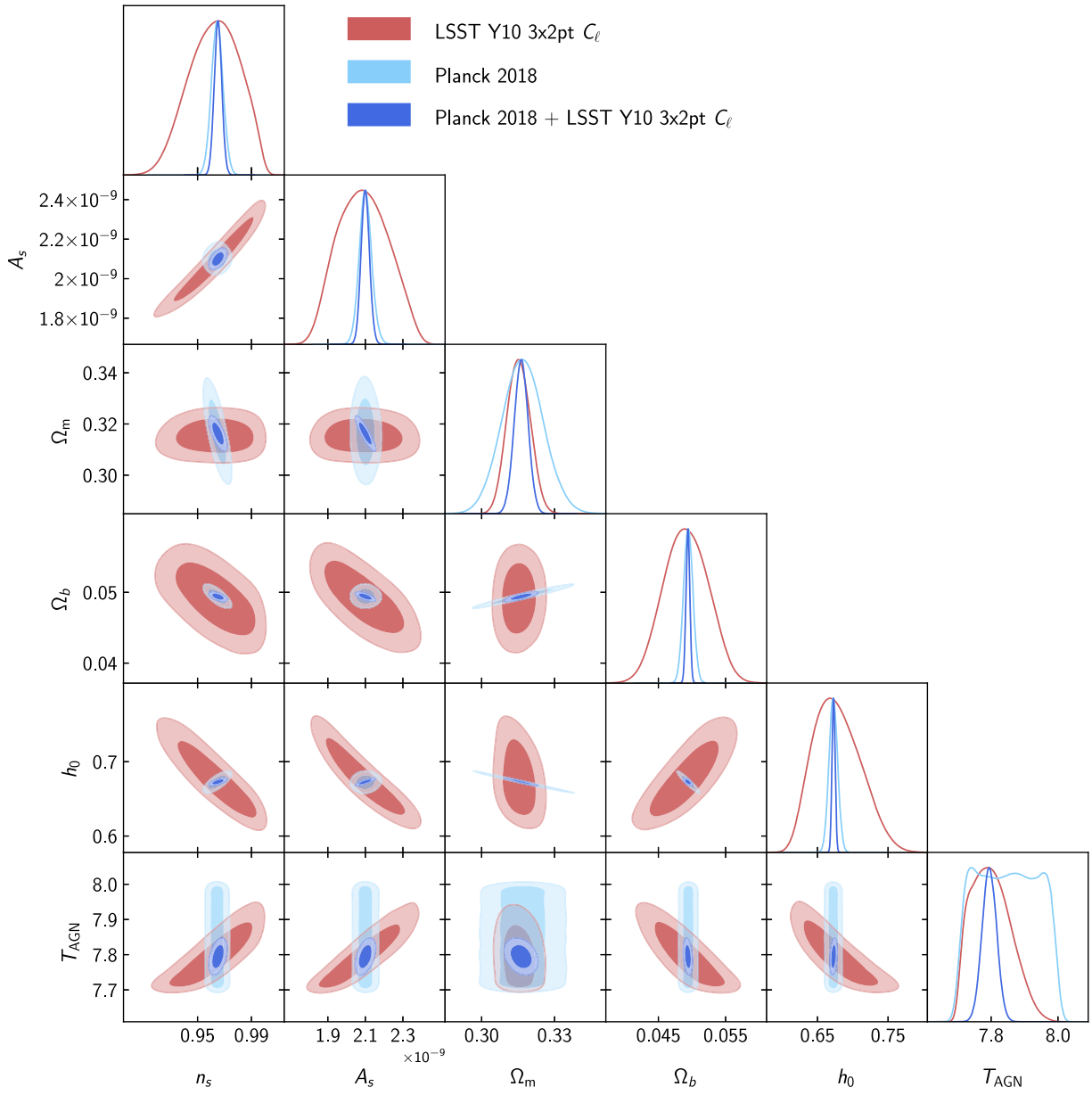

FIG. 4. Credible regions on cosmological parameters from our predicted LSST Y10 weak lensing and clustering data vector in harmonic space in ΛCDM in red along with constraints on corresponding parameters from *Planck* 2018 TTTEEE + low-ℓ + lensing likelihoods in light blue and their combination with LSST Y10 in blue.

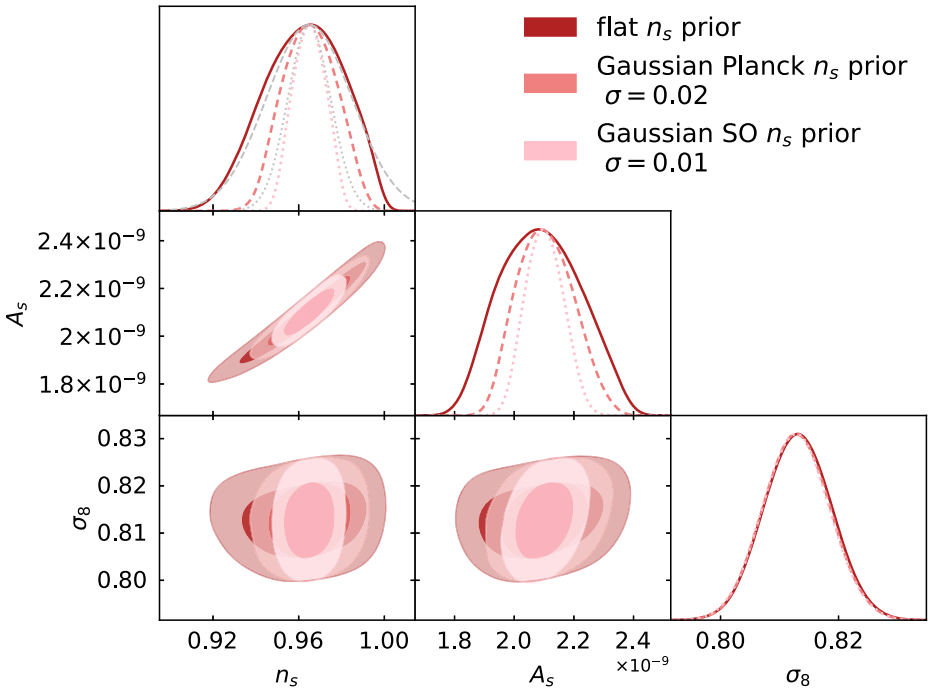

FIG. 5. Credible regions on the scalar spectral index n_s and amplitude A_s of scalar pertubations and σ_8 from our predicted LSST Y10 weak lensing and clustering data vector in harmonic space in red. In coral, we show the results from using a Gaussian prior with a width five times larger than *Planck* 2018 (i.e., $\sigma = 0.02$) on n_s, the prior is shown as a dashed gray line on the 1D n_s panel. We similarly show results from adding a Gaussian prior with a width five times larger than predicted from Simons Observatory (i.e., $\sigma = 0.01$) in pink, the prior is shown as a dotted gray line on the 1D n_s panel.

[1] L. Knox and M. S. Turner, Detectability of tensor perturbations through anisotropy of the cosmic background radiation, Phys. Rev. Lett. **73**, 3347 (1994).

[2] L. Knox, Determination of inflationary observables by cosmic microwave background anisotropy experiments, Phys. Rev. D **52**, 4307 (1995).

[3] S. Dodelson, W. H. Kinney, and E. W. Kolb, Cosmic microwave background measurements can discriminate among inflation models, Phys. Rev. D **56**, 3207 (1997).

[4] N. Aghanim, Y. Akrami, M. Ashdown, J. Aumont, C. Baccigalupi, M. Ballardini, A. J. Banday, R. B. Barreiro, N. Bartolo, S. Basak *et al.* (Planck Collaboration), Planck 2018 results—VI. Cosmological parameters, Astron. Astrophys. **641**, A6 (2020).

[5] P. A. R. Ade, Z. Ahmed, M. Amiri, D. Barkats, R. B. Thakur, C. A. Bischoff, D. Beck, J. J. Bock, H. Boenish, E. Bullock *et al.*, Improved constraints on primordial gravitational waves using Planck, WMAP, and BICEP/Keck observations through the 2018 observing season, Phys. Rev. Lett. **127**, 151301 (2021).

[6] E. Allys, K. Arnold, J. Aumont, R. Aurlien, S. Azzoni, C. Baccigalupi, A. J. Banday, R. Banerji, R. B. Barreiro, N. Bartolo *et al.* (LiteBIRD Collaboration), Probing cosmic inflation with the LiteBIRD cosmic microwave background polarization survey, Prog. Theor. Exp. Phys. **2023**, 042F01 (2022).

[7] P. Ade, J. Aguirre, Z. Ahmed, S. Aiola, A. Ali, D. Alonso, M. A. Alvarez, K. Arnold, P. Ashton, J. Austermann *et al.*, The Simons Observatory: Science goals and forecasts, J. Cosmol. Astropart. Phys. 02 (2019) 056.

[8] K. Abazajian, G. E. Addison, P. Adshead, Z. Ahmed, D. Akerib, A. Ali, S. W. Allen, D. Alonso, M. Alvarez, M. A. Amin *et al.*, CMB-S4: Forecasting constraints on primordial gravitational waves, Astrophys. J. **926**, 54 (2022).

[9] J. A. Tyson, Large synoptic survey telescope: Overview, in *Survey and Other Telescope Technologies and Discoveries*, edited by J. A. Tyson and S. Wolff (International Society for Optics and Photonics, SPIE, 2002), Vol. 4836, pp. 10–20, 10.1117/12.456772.

[10] Z. Ivezić (The LSST Science Collaboration), Large synoptic survey telescope science requirements document (2011), https://docushare.lsst.org/docushare/dsweb/Get/LPM-17.

[11] R. Laureijs, J. Amiaux, S. Arduini, J. L. Augueres, J. Brinchmann, R. Cole, M. Cropper, C. Dabin, L. Duvet, A. Ealet *et al.*, Euclid definition study report, arXiv: 1110.3193.

[12] R. Akeson, L. Armus, E. Bachelet, V. Bailey, L. Bartusek, A. Bellini, D. Benford, D. Bennett, A. Bhattacharya, R. Bohlin *et al.*, The wide field infrared survey telescope: 100 hubbles for the 2020s, arXiv:1902.05569.

[13] R. Mandelbaum, T. Eifler, R. Hložek, T. Collett, E. Gawiser, D. Scolnic, D. Alonso, H. Awan, R. Biswas *et al.* (The LSST Dark Energy Science Collaboration), The LSST Dark Energy Science Collaboration (DESC) science requirements document, arXiv:1809.01669.

[14] A. Ferté, D. Kirk, A. R. Liddle, and J. Zuntz, Testing gravity on cosmological scales with cosmic shear, cosmic microwave background anisotropies, and redshift-space distortions, Phys. Rev. D **99**, 083512 (2019).

[15] A. Blanchard, S. Camera, C. Carbone, V. F. Cardone, S. Casas, S. Clesse, S. Ilić, M. Kilbinger, T. Kitching, M. Kunz *et al.* (Euclid Collaboration), Euclid preparation. VII. Forecast validation for Euclid cosmological probes, Astron. Astrophys. **642**, A191 (2020).

[16] T. Eifler, H. Miyatake, E. Krause, C. Heinrich, V. Miranda, C. Hirata, J. Xu, S. Hemmati, M. Simet, P. Capak *et al.*, Cosmology with the Roman Space Telescope—Multiprobe strategies, Mon. Not. R. Astron. Soc. **507**, 1746 (2021).

[17] T. Abbott, M. Aguena, A. Alarcon, S. Allam, O. Alves, A. Amon, F. Andrade-Oliveira, J. Annis, S. Avila, D. Bacon *et al.*, Dark Energy Survey Year 3 results: Cosmological constraints from galaxy clustering and weak lensing, Phys. Rev. D **105**, 023520 (2022).

[18] S. More, S. Sugiyama, H. Miyatake, M. M. Rau, M. Shirasaki, X. Li, A. J. Nishizawa, K. Osato, T. Zhang, M. Takada *et al.*, Hyper Suprime-Cam Year 3 results: Measurements of clustering of SDSS-BOSS galaxies, galaxy-galaxy lensing and cosmic shear (2023).

[19] C. Heymans, T. Tröster, M. Asgari, C. Blake, H. Hildebrandt, B. Joachimi, K. Kuijken, C.-A. Lin, A. G. Sá nchez, J. L. van den Busch *et al.*, KiDS-1000 cosmology: Multi-probe weak gravitational lensing and spectroscopic galaxy clustering constraints, Astron. Astrophys. **646**, A140 (2021).

[20] A. Albrecht, G. Bernstein, R. Cahn, W. L. Freedman, J. Hewitt, W. Hu, J. Huth, M. Kamionkowski, E. W. Kolb, L. Knox, J. C. Mather, S. Staggs, and N. B. Suntzeff, Report of the dark energy task force, arXiv:astro-ph/0609591.

[21] T. Giannantonio, C. Porciani, J. Carron, A. Amara, and A. Pillepich, Constraining primordial non-Gaussianity with future galaxy surveys, Mon. Not. R. Astron. Soc. **422**, 2854 (2012).

[22] D. Yamauchi, K. Takahashi, and M. Oguri, Constraining primordial non-Gaussianity via a multitracer technique with surveys by Euclid and the square kilometre array, Phys. Rev. D **90**, 083520 (2014).

[23] O. Doré, M. W. Werner, M. L. N. Ashby, L. E. Bleem, J. Bock, J. Burt, P. Capak, T.-C. Chang, J. Chaves-Montero, C. H. Chen *et al.*, Science impacts of the SPHEREx all-sky optical to near-infrared spectral survey II: Report of a community workshop on the scientific synergies between the SPHEREx survey and other astronomy observatories (2018).

[24] S. Hilbert, L. Marian, R. E. Smith, and V. Desjacques, Measuring primordial non-Gaussianity with weak lensing surveys, Mon. Not. R. Astron. Soc. **426**, 2870 (2012).

[25] F. Schmidt, N. E. Chisari, and C. Dvorkin, Imprint of inflation on galaxy shape correlations, J. Cosmol. Astropart. Phys. 10 (2015) 032.

[26] M. Gatti, C. Chang, O. Friedrich, B. Jain, D. Bacon, M. Crocce, J. DeRose, I. Ferrero, P. Fosalba, E. Gaztanaga *et al.*, Dark Energy Survey Year 3 results: Cosmology with moments of weak lensing mass maps—Validation on simulations, Mon. Not. R. Astron. Soc. **498**, 4060 (2020).

[27] J. Prat, J. Zuntz, C. Chang, T. Tröster, E. Pedersen, C. Garcí a-García, E. Phillips-Longley, J. Sanchez, D. Alonso, X. Fang *et al.*, The catalog-to-cosmology framework for weak lensing and galaxy clustering for LSST, Open J. Astrophys. **6** (2023).10.21105/astro.2212.09345

[28] T. Tan, D. Zürcher, J. Fluri, A. Refregier, F. Tarsitano, and T. Kacprzak, Assessing theoretical uncertainties for cosmological constraints from weak lensing surveys, Mon. Not. R. Astron. Soc. **522**, 3766 (2023).

[29] D. Chandra and S. Pal, Investigating the constraints on primordial features with future cosmic microwave background and galaxy surveys, J. Cosmol. Astropart. Phys. 09 (2022) 024.

[30] Z. Huang, L. Verde, and F. Vernizzi, Constraining inflation with future galaxy redshift surveys, J. Cosmol. Astropart. Phys. 04 (2012) 005.

[31] C. Sánchez, J. Prat, G. Zacharegkas, S. Pandey, E. Baxter, G. Bernstein, J. Blazek, R. Cawthon, C. Chang, E. Krause *et al.*, Dark Energy Survey Year 3 results: Exploiting small-scale information with lensing shear ratios, Phys. Rev. D **105**, 083529 (2022).

[32] A. Lewis and S. Bridle, Cosmological parameters from CMB and other data: A Monte Carlo approach, Phys. Rev. D **66**, 103511 (2002).

[33] A. Lewis, A. Challinor, and A. Lasenby, Efficient computation of CMB anisotropies in closed FRW models, Astrophys. J. **538**, 473 (2000).

[34] C. Howlett, A. Lewis, A. Hall, and A. Challinor, CMB power spectrum parameter degeneracies in the era of precision cosmology, J. Cosmol. Astropart. Phys. 04 (2012) 027.

[35] A. Lewis, CAMB notes, https://cosmologist.info/notes/CAMB.pdf.

[36] A. J. Mead, S. Brieden, T. Tröster, and C. Heymans, HMCode-2020: Improved modelling of non-linear cosmological power spectra with baryonic feedback, Mon. Not. R. Astron. Soc. **502**, 1401 (2021).

[37] S. Bridle and L. King, Dark energy constraints from cosmic shear power spectra: Impact of intrinsic alignments on photometric redshift requirements, New J. Phys. **9**, 444 (2007).

[38] E. Krause, T. F. Eifler, J. Zuntz, O. Friedrich, M. A. Troxel, S. Dodelson, J. Blazek, L. F. Secco, N. MacCrann, E. Baxter *et al.*, Dark Energy Survey Year 1 results: Multi-probe methodology and simulated likelihood analyses, arXiv:1706.09359.

[39] J. Zuntz, M. Paterno, E. Jennings, D. Rudd, A. Manzotti, S. Dodelson, S. Bridle, S. Sehrish, and J. Kowalkowski, CosmoSIS: Modular cosmological parameter estimation, Astron. Comput. **12**, 45 (2015).

[40] J. U. Lange, NAUTILUS: Boosting Bayesian importance nested sampling with deep learning, arXiv:2306.16923.

[41] A. J. Ross, L. Samushia, C. Howlett, W. J. Percival, A. Burden, and M. Manera, The clustering of the SDSS DR7 main galaxy sample—I. A 4 per cent distance measure at $z = 0.15$, Mon. Not. R. Astron. Soc. **449**, 835 (2015).

[42] S. Alam, M. Ata, S. Bailey, F. Beutler, D. Bizyaev, J. A. Blazek, A. S. Bolton, J. R. Brownstein, A. Burden, C.-H. Chuang *et al.*, The clustering of galaxies in the completed SDSS-III baryon oscillation spectroscopic survey: Cosmological analysis of the DR12 galaxy sample, Mon. Not. R. Astron. Soc. **470**, 2617 (2017).

[43] S. Alam, M. Aubert, S. Avila, C. Balland, J. E. Bautista, M. A. Bershady, D. Bizyaev, M. R. Blanton, A. S. Bolton, J. Bovy *et al.*, Completed SDSS-IV extended baryon oscillation spectroscopic survey: Cosmological implications from two decades of spectroscopic surveys at the apache point observatory, Phys. Rev. D **103**, 083533 (2021).

[44] J. E. Bautista, R. Paviot, M. Vargas Magaña, S. de la Torre, S. Fromenteau, H. Gil-Marín, A. J. Ross, E. Burtin, K. S. Dawson, J. Hou *et al.*, The completed SDSS-IV extended Baryon Oscillation Spectroscopic Survey: Measurement of the BAO and growth rate of structure of the luminous red galaxy sample from the anisotropic correlation function between redshifts 0.6 and 1, Mon. Not. R. Astron. Soc. **500**, 736 (2021).

[45] H. Gil-Marín, J. E. Bautista, R. Paviot, M. Vargas-Magaña, S. de la Torre, S. Fromenteau, S. Alam, S. Ávila, E. Burtin, C.-H. Chuang *et al.*, The completed SDSS-IV extended Baryon Oscillation Spectroscopic Survey: Measurement of the BAO and growth rate of structure of the luminous red galaxy sample from the anisotropic power spectrum between redshifts 0.6 and 1.0, Mon. Not. R. Astron. Soc. **498**, 2492 (2020).

[46] A. de Mattia, V. Ruhlmann-Kleider, A. Raichoor, A. J. Ross, A. Tamone, C. Zhao, S. Alam, S. Avila, E. Burtin, J. Bautista *et al.*, The completed SDSS-IV extended Baryon Oscillation Spectroscopic Survey: Measurement of the BAO and growth rate of structure of the emission line galaxy sample from the anisotropic power spectrum between redshift 0.6 and 1.1, Mon. Not. R. Astron. Soc. **501**, 5616 (2021).

[47] R. Neveux, E. Burtin, A. de Mattia, A. Smith, A. J. Ross, J. Hou, J. Bautista, J. Brinkmann, C.-H. Chuang, K. S. Dawson *et al.*, The completed SDSS-IV extended Baryon Oscillation Spectroscopic Survey: BAO and RSD measurements from the anisotropic power spectrum of the quasar sample between redshift 0.8 and 2.2, Mon. Not. R. Astron. Soc. **499**, 210 (2020).

[48] J. Hou, A. G. Sá nchez, A. J. Ross, A. Smith, R. Neveux, J. Bautista, E. Burtin, C. Zhao, R. Scoccimarro, K. S. Dawson *et al.*, The completed SDSS-IV extended Baryon Oscillation Spectroscopic Survey: BAO and RSD measurements from anisotropic clustering analysis of the quasar sample in configuration space between redshift 0.8 and 2.2, Mon. Not. R. Astron. Soc. **500**, 1201 (2020).

[49] H. du Mas des Bourboux, J. Rich, A. Font-Ribera, V. de Sainte Agathe, J. Farr, T. Etourneau, J.-M. Le Goff, A. Cuceu, C. Balland, J. E. Bautista *et al.*, The completed SDSS-IV extended Baryon Oscillation Spectroscopic Survey: Baryon acoustic oscillations with Lyα forests, Astrophys. J. **901**, 153 (2020).

[50] A. Lewis, GetDist: A Python package for analysing Monte Carlo samples, arXiv:1910.13970.

[51] K. T. Story, C. L. Reichardt, Z. Hou, R. Keisler, K. A. Aird, B. A. Benson, L. E. Bleem, J. E. Carlstrom, C. L. Chang, H.-M. Cho *et al.*, A measurement of the cosmic microwave background samping tail from the 2500-square-degree SPT-SZ survey, Astrophys. J. **779**, 86 (2013).

[52] G. Hinshaw, D. Larson, E. Komatsu, D. N. Spergel, C. L. Bennett, J. Dunkley, M. R. Nolta, M. Halpern, R. S. Hill, N. Odegard *et al.*, Nine-year Wilkinson microwave anisotropy probe (WMAP) observations: Cosmological parameter results, Astrophys. J. Suppl. Ser. **208**, 19 (2013).

[53] A. A. Starobinsky, Spectrum of adiabatic perturbations in the universe when there are singularities in the inflationary potential, Sov. J. Exp. Theor. Phys. Lett. **55**, 489 (1992), http://jetpletters.ru/ps/1276/article_19291.shtml.

[54] A. A. Starobinsky, A new type of isotropic cosmological models without singularity, Phys. Lett. **91B**, 99 (1980).

[55] V. F. Mukhanov and G. V. Chibisov, Quantum fluctuations and a nonsingular universe, Sov. J. Exp. Theor. Phys. Lett. **33**, 532 (1981), http://jetpletters.ru/ps/1510/article_23079.shtml.

[56] S. Joudaki, A. Mead, C. Blake, A. Choi, J. de Jong, T. Erben, I. Fenech Conti, R. Herbonnet, C. Heymans, H. Hildebrandt, H. Hoekstra, B. Joachimi, D. Klaes, F. Köhlinger, K. Kuijken, J. McFarland, L. Miller, P. Schneider, and M. Viola, Kids-450: Testing extensions to the standard cosmological model, Mon. Not. R. Astron. Soc. **471**, 1259 (2017).